Dynamic Evolution of Interface Roughness During Friction and Wear Processes

Kubiak, K. J.; Bigerelle, M.; Mathia, T. G.; Dubois, A.; Dubar, L.

Published in:
Scanning

DOI:
10.1002/sca.21082

Publication date:
2014

SCANNING VOL. 36, 30–38 (2014)

Dynamic Evolution of Interface Roughness During Friction and Wear Processes

K.J. Kubiak,[1,2] M. Bigerelle,[2,4] T.G. Mathia,[3] A. Dubois,[2,4] and L. Dubar[2,4]

[1]University of Leeds, School of Mechanical Engineering, Institute of Engineering Thermofluids, Surfaces and Interfaces (iETSI), Leeds, United Kingdom
[2]Université de Valenciennes et du Hainaut-Cambrésis, TEMPO EA 4542, Valenciennes Cedex 9, France
[3]Ecole Centrale de Lyon, Laboratoire de Tribologie et Dynamique des Systèmes (LTDS UMR 5513 CNRS), Ecully, France
[4]PRES Lille, Nord de France

Summary: Dynamic evolution of surface roughness and influence of initial roughness (S_a = 0.282–6.73 μm) during friction and wear processes has been analyzed experimentally. The mirror polished and rough surfaces (28 samples in total) have been prepared by surface polishing on Ti–6Al–4V and AISI 1045 samples. Friction and wear have been tested in classical sphere/plane configuration using linear reciprocating tribometer with very small displacement from 130 to 200 μm. After an initial period of rapid degradation, dynamic evolution of surface roughness converges to certain level specific to a given tribosystem. However, roughness at such dynamic interface is still increasing and analysis of initial roughness influence revealed that to certain extent, a rheology effect of interface can be observed and dynamic evolution of roughness will depend on initial condition and history of interface roughness evolution. Multiscale analysis shows that morphology created in wear process is composed from nano, micro, and macro scale roughness. Therefore, mechanical parts working under very severe contact conditions, like rotor/blade contact, screws, clutch, etc. with poor initial surface finishing are susceptible to have much shorter lifetime than a quality finished parts. SCANNING 36: 30–38, 2014. © 2013 Wiley Periodicals, Inc.

Key words: surface roughness evolution, dynamic roughness, dry friction, roughness metrology, surface finishing

Introduction

Initial surface roughness can have significant influence on friction and wear processes in tribological contacts under fretting conditions (Kubiak and Mathia, 2009; Sokoloff *et al*., 2012; Stahlmann *et al*., 2012). Damage induced by fretting is considered as a plague for modern industry and can be found in many engineering applications (Fu *et al*., 1998) for example in transport industry, electrical contacts, bridge cable lines, rotor/blade contact of jet engine, but also in dental implants and brackets (Rapiejko *et al*., 2009), hip and knee prosthesis. Degradation of such contact is a dynamic process and conditions at interface are constantly changing (Jerier and Molinari, 2012). Wear process, abrasion in contact and creation of third body will influence dynamic evolution of interface roughness. For very severe contact conditions (Kasarekar *et al*., 2008) often encountered in fretting, initial surface will be totally removed and newly created surface will usually be very complex due to physical and chemical processes taking place at interface. Therefore, multiscale analysis approach should be used to evaluate interface morphology. Along with statistical parameters, used to evaluate roughness height and spatial characteristic, many researchers started to use multiscale decomposition method (Bouchbinder *et al*., 2006; Bigerelle *et al*., 2007, 2012). Fourier transform, wavelet transformation and fractal methods are more often used (Brown and Siegmann, 2001; Ungar *et al*., 2003; Kang *et al*., 2005; Scott *et al*., 2005). Taking into account multiscale roughness of interface and dynamic nature of friction and wear processes, it is important to analyze the interface roughness evolution during sliding and wear (Elliott *et al*., 1998). From a practical point of view, initial roughness in manufacturing process is much easier to control. It is frequently used to obtain specific functionalities of final parts and components. Therefore, in this article we will focus on initial roughness and its influence on friction and wear process dynamics.

Contract grant sponsor: Laboratory TEMPO, University of Valenciennes, Valenciennes, France.

Address for reprints: K.J. Kubiak, University of Leeds, School of Mechanical Engineering, Institute of Engineering Thermofluids, Surfaces and Interfaces (iETSI), Woodhouse Lane, Leeds LS2 9JT, United Kingdom
E-mail: krzysztof@kubiak.co.uk

Received 18 July 2012; Accepted with revision 11 January 2013

DOI 10.1002/sca.21082
Published online 25 February 2013 in Wiley Online Library (wileyonlinelibrary.com).

Experimental Procedure

Tested Materials

Two commonly used engineering materials were selected in this study: low carbon alloy (AISI 1045) and titanium alloy (Ti–6Al–4V). Two relatively hard materials were selected as counterbodies to simplify analysis and avoid high wear rate: AISI 52100 ball bearing steel and Al_2O_3 ceramic ball. For analysis of initial roughness influence and dynamic evolution of interface roughness the plane specimens AISI 1045 were tested against AISI 52100 ball and a plane Ti–6Al–4V specimens against ceramic ball.

Rough Surface Preparation

The experimental specimens were machined into small rectangular blocks and they were polished to obtain an uniform roughness on their working surface. Subsequently different grit size were involved to produce surfaces with S_a roughness ranging from 0.035 to 6.73 μm. Tests performed to analyze dynamic evolution of surface roughness were carried out directly on the "almost mirror" polished surfaces with $S_a = 0.035$ μm. However, influence of initial surface roughness was also investigated using specimens with different initial roughness ranging from $S_a = 0.282$ to 6.73 μm. Commercially available spheres from ball bearing were used as counterbodies, they are characterized by smooth surface of about $S_a = 0.2$ μm and no additional treatment were used in this case.

Preparation of the surface by abrasive polishing can generate initial compressive residual stress near to the surface. However, high local contact stress during fretting will lead to relaxation of initial residual stress after few cycles in gross slip regime (Kubiak *et al.*, 2010) when whole contact area is subjected to relative sliding. Therefore, in this study carried out in gross slip regime, the initial residual stress will not be taken into account.

Surface Roughness Measurements

The initially polished surfaces and the specimens with different initial roughness prepared on AISI 1045 and Ti–6Al–4V were measured by Wyko NT3300S optical interferometric profiler. Vertical Scanning Interferometry (VSI) mode was used to measure the surfaces. The measurement principle is that unfiltered white light beam is split in two. Half of a beam is directed through a microscope objective and reflected from the surface and half is reflected from the reference mirror. When reflected beams combine together they produce interference fringes, where the best-contrast fringe occurs at best focus. In VSI mode the objective moves vertically to scan the surface at various heights. A 3D surface is reconstructed by analysis of fringes at every pixel. VSI mode uses algorithms to process fringe modulation data from the intensity signal to calculate surface heights. In our measurements an objective with 5× magnification was used and resulting sampling of obtained profile was 1.6 μm in X and Y direction and vertical resolution was 10 nm. For results consistency all measurements were done in VSI mode. All the surfaces were anisotropic and sliding direction between plane and sphere was perpendicular to the initial surface texture. Examples of measured 3D topologies on AISI 1045 and Ti–6Al–4V material are presented in Figure 1. It can be noted that an initial anisotropic surface roughness has been totally removed from the surface during a wear process. Traces of fretting reveals abrasive character of fretting wear and presence of third body in the contact causing very deep scratches in center of wear trace. More abrasive character can be observed for titanium alloy.

Experimental Setup for Friction and Wear Tests

The experimental analysis of initial surface roughness influence on friction, wear, and dynamic evolution of interface morphology were carried out using linear micro-displacement tribometer (Kubiak *et al.*, 2011). Reciprocating displacement motion with a frequency F of 15 Hz is generated by electrodynamic shaker. Test is controlled by imposing constant displacement. Figure 2 shows schematic diagram of used tribometer and interface contact configuration. During the tests, normal load in the contact was applied by fixed mass and was kept constant at $P = 10$ and 20 N. Tangential force (Q) and relative displacement (δ) were recorded continuously, using that signals, various tribological parameters can be calculated and displacement amplitude is used in feedback loop to keep displacement amplitude constant during the test (Kubiak *et al.*, 2005, 2006).

Results and Discussion

Friction and wear are complex phenomena involving physical and chemical interactions of interface and also mechanical deformations of near surface material. During dry contact friction, even for the conditions involving only elastic contact deformation in macroscopic scale, due to roughness of real surface, contact between two solids take place first on asperities peaks. Stress distribution in local contact spots can however exceed the elastic limit and materials on a smaller scale will be deformed plastically. Therefore, by controlling surface morphology one can control how the contact between solids will take place.

Dynamic Evolution of Roughness During Wear Process

Dynamic evolution of surface morphology has been evaluated by analysis of surface profiles after tests with

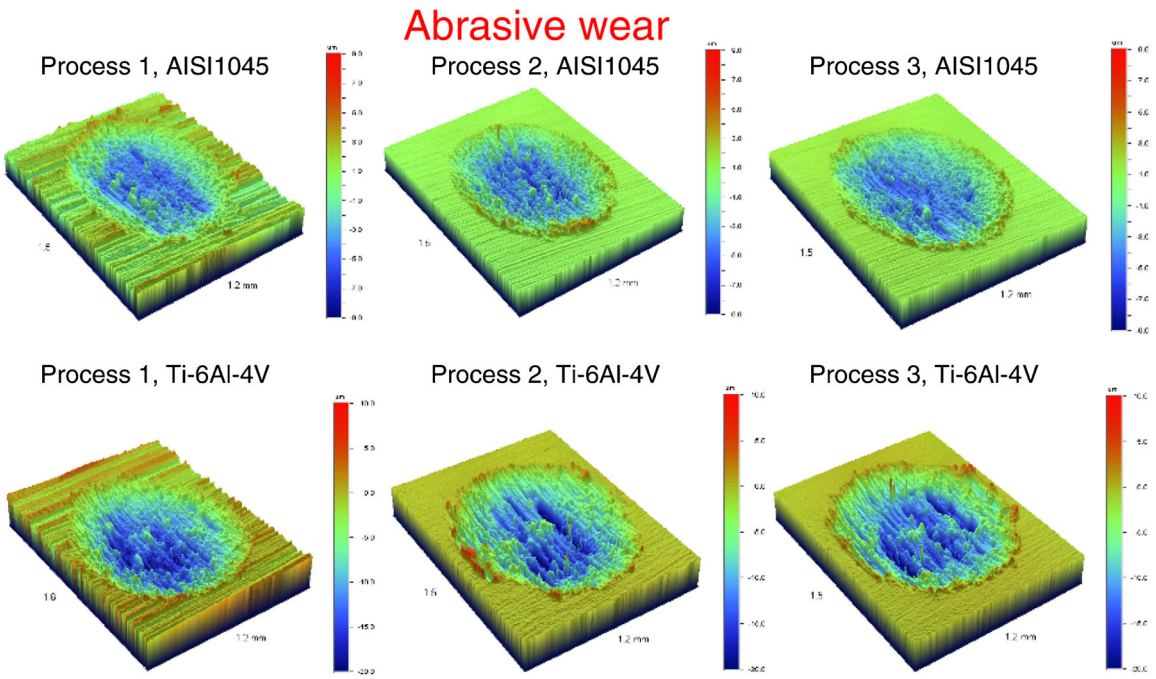

Fig 1. 3D morphologies with different initial surface roughness (Processes 1, 2 and 3) prepared by abrasive polishing on a low carbon alloy AISI 1045 and titanium alloy Ti–6Al–4V. Test conditions: $P = 10$ N, $\delta^* = 200$ µm, $F = 15$ Hz, $N = 5{,}000$ cycles, contact configuration plane/sphere AISI 1045/AISI 52100 and Ti–6Al–4V/Al_2O_3 respectively.

different number of cycles. Initially mirror polished surface of Ti–6Al–4V has been tested in sphere/plane configuration for 2,000, 5,000, 7,500, and 10,000 cycles. Profiles of worn plane surface in direction perpendicular to sliding direction are plotted in Figure 3. Spherical shape of wear scars has been removed from profile and only roughness is plotted and analyzed. Already after the first 2,000 cycles, a

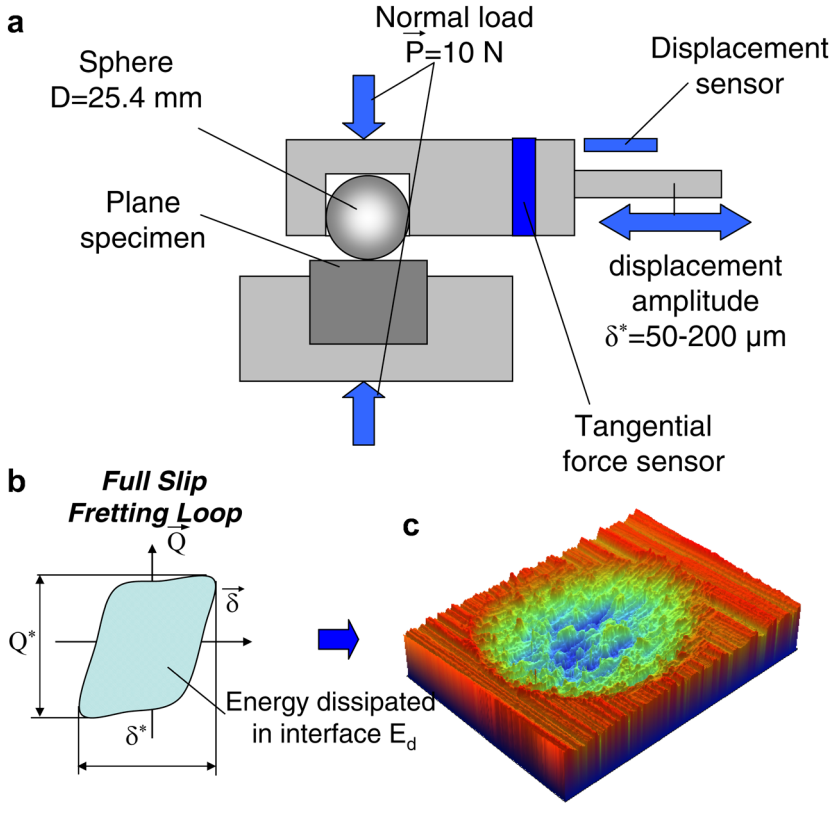

Fig 2. Fretting test: (**a**) contact configuration, (**b**) fretting loop, and (**c**) fretting wear scar (Ti–6Al–4V) (after Kubiak *et al.*, 2011).

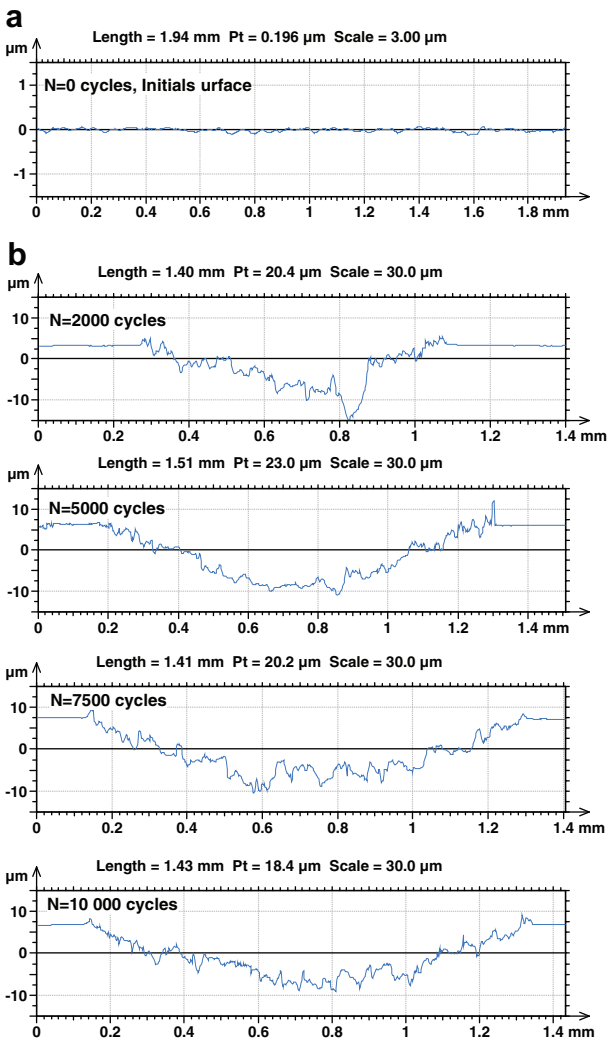

Fig 3. Dynamic evolution of roughness profiles during wear process, 2D profile taken in a middle cross section in direction perpendicular to contact sliding direction (**a**) initial profile, (**b**) wear trace (plane material Ti–6Al–4V, $P = 20$ N, $\delta^* = 130$ µm, $F = 15$ Hz).

significant surface degradation and increase in roughness can be observed. Summary of roughness parameters evolution can be found in Table I. Slight increase in roughness can be observed between 2,000 and 5,000 cycles, but no further degradation was observed for this configuration. Note that tests were performed on mirror polished surface and therefore influence of initial roughness is very limited in this case and each test will have similar rheological history. Evolution of wear on sphere counterbodies have similar tendency to evolution on plane surface. Observed wear has abrasive character and after initial period of intensive degradation, an equilibrium state between material removal from peaks and valleys of asperities is reached. Roughness of interface will in this case slightly increase but it is already at very high level.

TABLE I Dynamic evolution of surface morphology during wear process, measured at different number of cycles in a wear trace on surface with removed spherical form and filtered with Gaussian filter 0.08 mm (plane material Ti–6Al–4V, $P = 20$ N, $\delta^* = 130$ µm, $F = 15$ Hz)

Cycles	Initial	2,000	5,000	7,000	10,000
Height parameters					
S_q (µm)	0.045	2.09	1.82	1.5	1.56
S_{sk}	0.229	−0.249	−0.214	−0.228	−0.802
S_{ku}	3.23	3.77	5.05	3.27	5.16
S_p (µm)	0.197	15.3	19.9	12.4	12.9
S_v (µm)	0.272	15.3	23.1	16.5	17.2
S_z (µm)	0.47	30.6	43	28.9	30.2
S_a (µm)	0.035	1.61	1.43	1.22	1.23
Functional parameters					
S_{mc} (µm)	0.058	2.66	2.17	1.97	1.87
S_{xp} (µm)	0.083	4.72	4.05	3.04	3.52
Feature parameters					
S_{pd} (1/mm^2)	277	184	94.7	137	113
S_{pc} (1/mm)	7.81	319	547	324	422
S_{10z} (µm)	0.32	23.5	31.4	18.7	25
S_{5p} (µm)	0.12	10.3	16.1	9.14	9.51
S_{5v} (µm)	0.20	13.2	15.3	9.56	15.5

Influence of Initial Surface Roughness on Dynamic Evolution of Interface

Influence of initial roughness on dynamic evolution of interface morphology was analyzed on specimens prepared on AISI 1045 and Ti–6Al–4V material with different initial roughness. In this case, tests were carried out against AISI 52100 sphere. Profiles of the middle cross section of wear scars on Ti–6Al–4V measured in direction perpendicular to sliding direction are presented in Figure 4. Three surfaces with different initial roughness can be directly

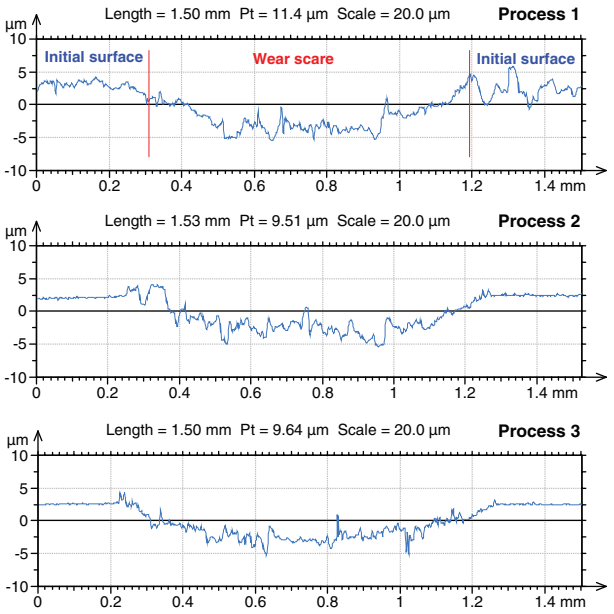

Fig 4. 2D profiles of fretting wear scar, middle plane perpendicular to sliding direction at maximum wear depth, material Ti–6Al–4V, for displacement amplitude 200 µm.

TABLE II Roughness parameters measured on initial surface and inside of wear scars, spherical form of wear scar have been removed and Gaussian filter 0.08 were used, material Ti–6Al–4V, $P = 10$ N, $\delta^* = 200$ µm, $N = 5{,}000$ cycles, $F = 15$ Hz

	Initial surface			Wear trace		
Process#	1	2	3	1	2	3
Height parameters						
S_q (µm)	1.43	0.441	0.365	1.88	2.41	2.92
S_p (µm)	6.48	2.2	2.06	14.4	16.4	15.4
S_v (µm)	6.73	1.61	1.71	10.7	11.2	19.6
S_z (µm)	13.2	3.81	3.77	25.1	27.5	35.1
S_a (µm)	1.11	0.339	0.282	1.43	1.89	2.14
Functional parameters						
S_{mc} (µm)	1.79	0.554	0.459	2.3	2.76	3.13
S_{xp} (µm)	3.13	0.82	0.667	3.85	5.55	7.97
Feature parameters						
S_{pd} (1/mm^2)	280	827	986	314	294	194
S_{pc} (1/mm)	51.9	31.3	29.3	398	436	412
S_{10z} (µm)	7.25	3.33	3.17	18.7	22.7	31.1
S_{5p} (µm)	3.83	1.85	1.81	10.4	14.5	14.4
S_{5v} (µm)	3.41	1.48	1.36	8.29	8.22	16.7

TABLE III Roughness parameters measured on initial surface and inside of wear scars, spherical form of wear scar have been removed and Gaussian filter 0.08 were used, material AISI 1045, $P = 10$ N, $\delta^* = 200$ µm, $N = 5{,}000$ cycles, $F = 15$ Hz

	Initial surface			Wear trace		
Process#	1	2	3	1	2	3
Height parameters						
S_q (µm)	2.88	0.52	0.377	0.974	1.02	0.792
S_p (µm)	11.7	2.5	2.07	9.19	6.19	3.51
S_v (µm)	15.7	2.46	1.46	6.09	5.23	4.19
S_z (µm)	27.4	4.97	3.53	15.3	11.4	7.7
S_a (µm)	2.16	0.409	0.282	0.712	0.756	0.593
Functional parameters						
S_{mc} (µm)	3.24	0.662	0.466	1.11	1.24	0.93
S_{xp} (µm)	7	0.982	0.689	1.84	2.02	1.68
Feature parameters						
S_{pd} (1/mm^2)	107	800	741	492	437	749
S_{pc} (1/mm)	78.1	35	27.7	337	136	118
S_{10z} (µm)	11.4	3.82	3.17	11.9	8.8	5.62
S_{5p} (µm)	4.72	1.95	1.88	7.52	4.67	2.56
S_{5v} (µm)	6.72	1.87	1.29	4.4	4.13	3.05

compared after the test with identical tribological conditions. Summary of roughness parameters measured inside the fretting scars is presented in Tables II and III for Ti–6Al–4V and AISI 1045 material respectively.

It can be noted that there are differences in the surface roughness inside the fretting traces after the test. They are related to initial surface roughness. This confirms that the rheological evolution and

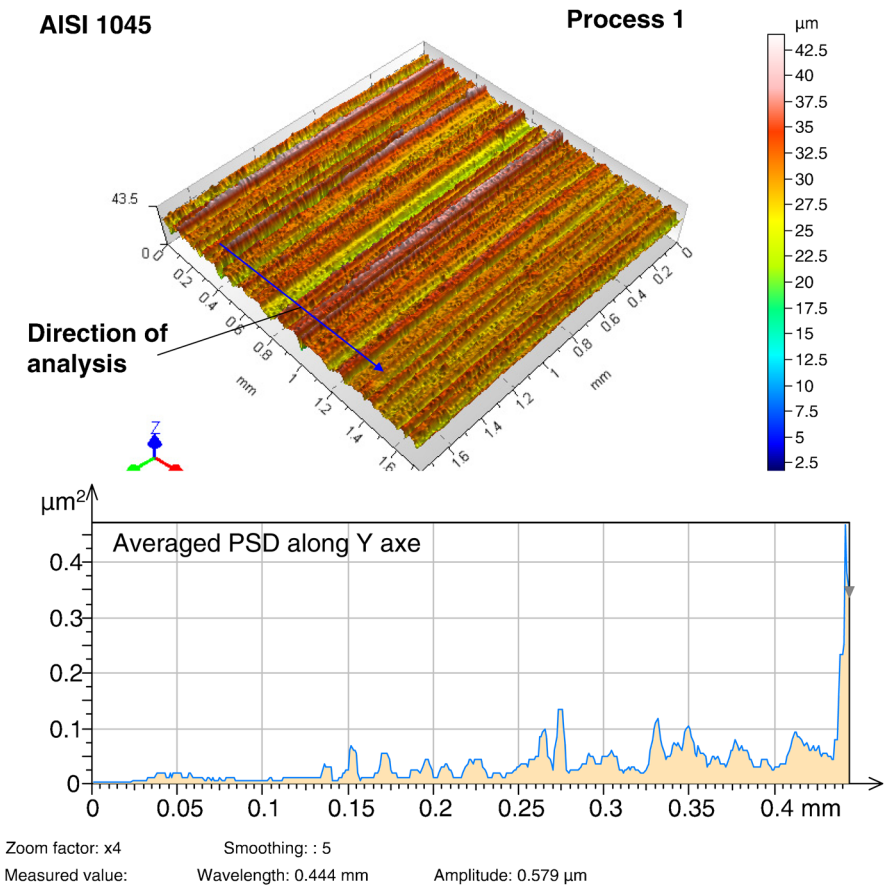

Fig 5. Surface morphology and Averaged Power Spectral Density function of AISI 1045 (Process 1) surface before a test.

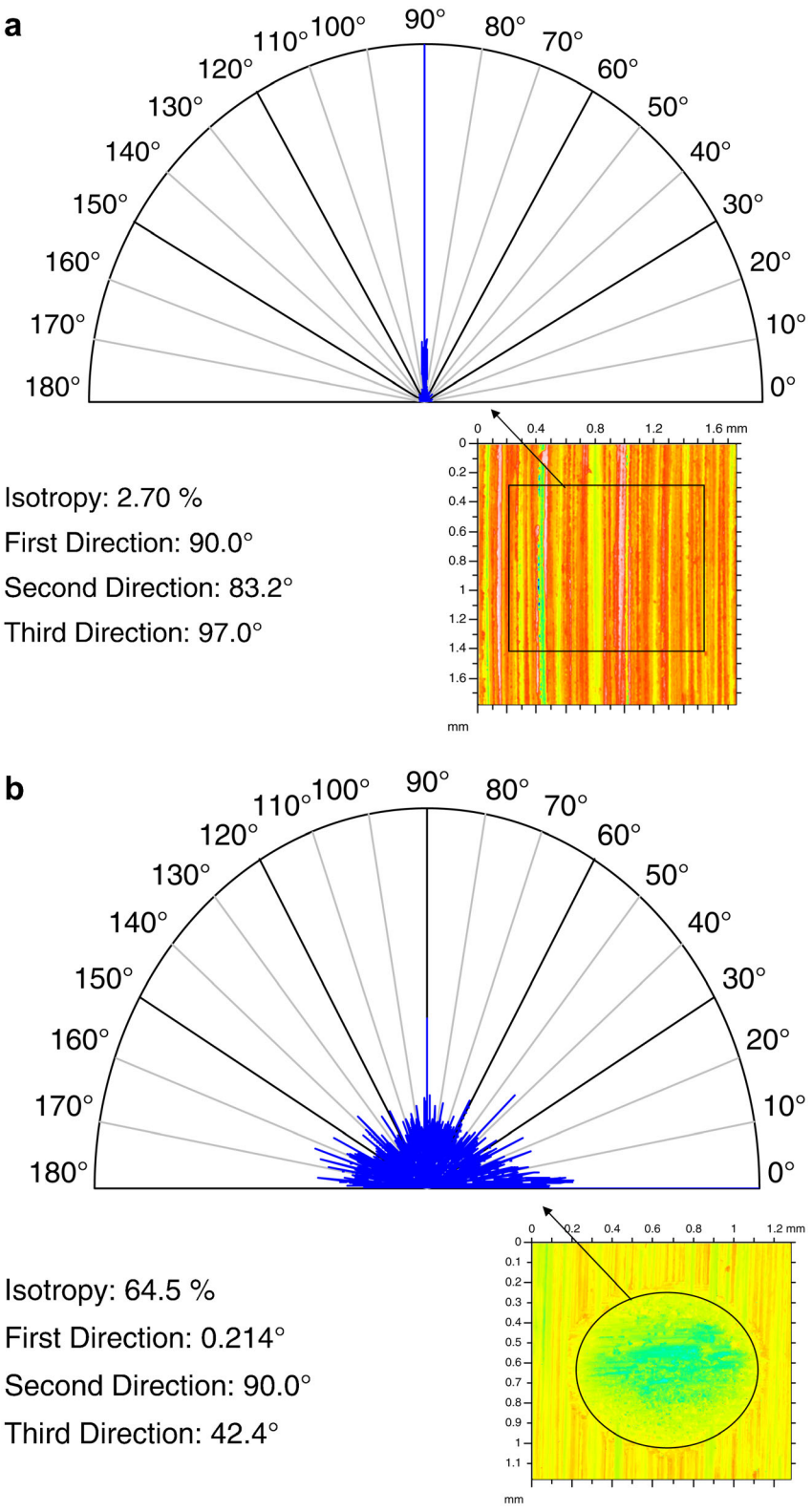

Fig 6. Analysis of texture direction of (**a**) initial and (**b**) worn interface roughness and its variation during fretting test with AISI 1045, $P = 10$ N, $\delta^* = 150$ µm, $F = 15$ Hz, $N = 5{,}000$ cycles.

history of the contact degradation have an influence on friction and wear processes. However, influence of the material and microstructure should be further investigated.

Multiscale Power Spectral Density Analysis

Further analyses of interface evolution during friction process were carried out using power spectral density

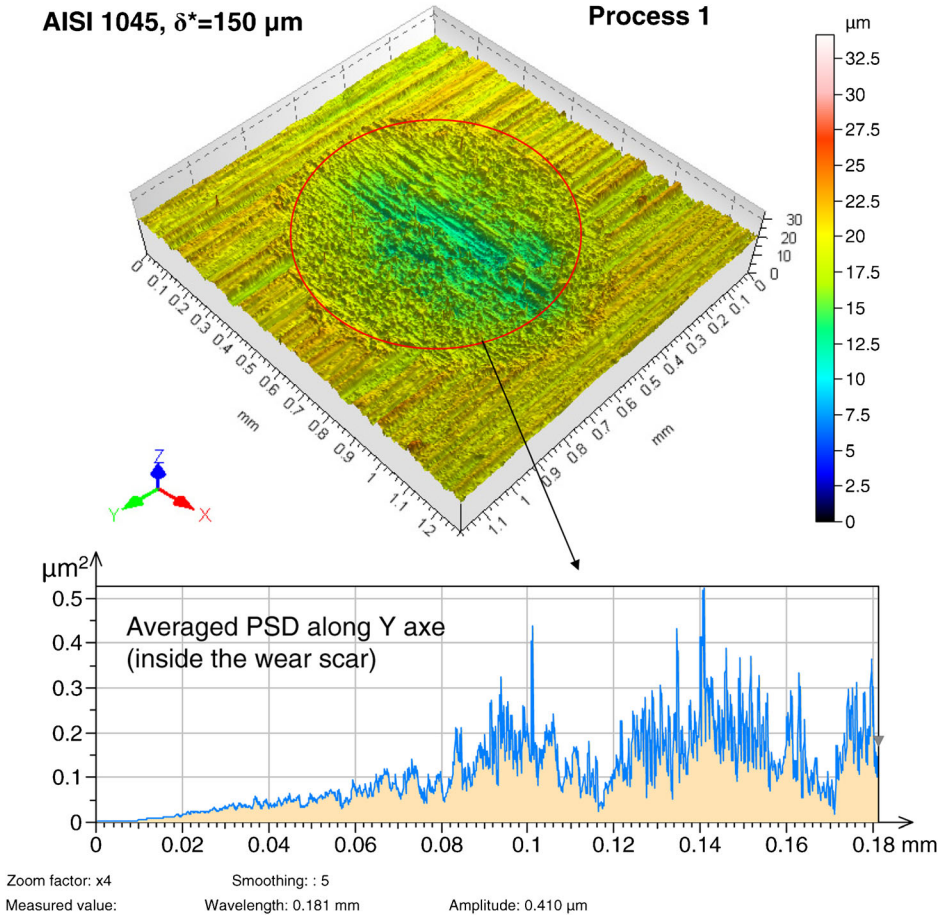

Fig 7. Power spectral density analysis of AISI 1045 (Process 1) surface after the test with $P = 10$ N, $\delta^* = 150$ μm, $F = 15$ Hz, $N = 5{,}000$ cycles.

analysis on 3D measured initial and worn surfaces. It represents a square value of amplitudes of surface roughness profiles as a function of wavelength. In this case, an averaged value of the consecutives lines of 3D surface is represented. Therefore, obtained spectrum will depend on the direction of analysis.

Multilevel analysis is revealing important changes in distribution of Power Spectral Density function on initial roughness and morphology created during wear process. Initial surface morphology prepared by abrasive polishing is composed from frequencies corresponding to the wavelength, i.e. peaks on PSD graph in Figure 5. These kind of dominant frequencies are likely to indicate surface anisotropy, which in this case is very high and only 2.7% of isotropy, has been calculated on initial surface (Fig. 6). Isotropy in tribological contact is increasing during the fretting test and after 5,000 cycles is about 64.5% (Fig. 6). Sliding direction is perpendicular to initial surface roughness texture and as it can be observed in Figures 5 and 7 due to wear process initial surface is totally removed and new rough surface is created. However, this is a very dynamic process and final roughness of interface will depend on the history of contact and roughness evolution during the friction process.

The results of PSD obtained for initial surface morphology are rather intuitive and they are similar for other surfaces prepared by polishing and other unidirectional processes like milling or turning, where rather single motif corresponding to the tool feed step, will be dominant in PSD distribution.

Multiscale analysis of surface morphology inside the fretting scar shows increasing and regularly distributed Power Spectral Density function with tendency to reduce the maximum wavelength in spectrum (Fig. 7). This means that morphology created in wear process is composed from nano, micro, and macro scale roughness. Therefore, abrasive wear process take place at all scale levels. Analyzing obtained PSD for worn surface, one can expect to find self-similarity at different levels. Figure 8(a,b) confirm that hypothesis showing similar roughness profiles of surface created by abrasive wear process at different scale levels. Isotropy of worn surface is increasing comparing to initial surface, however first direction of motives change from initial polishing direction to direction of sliding of interfaces.

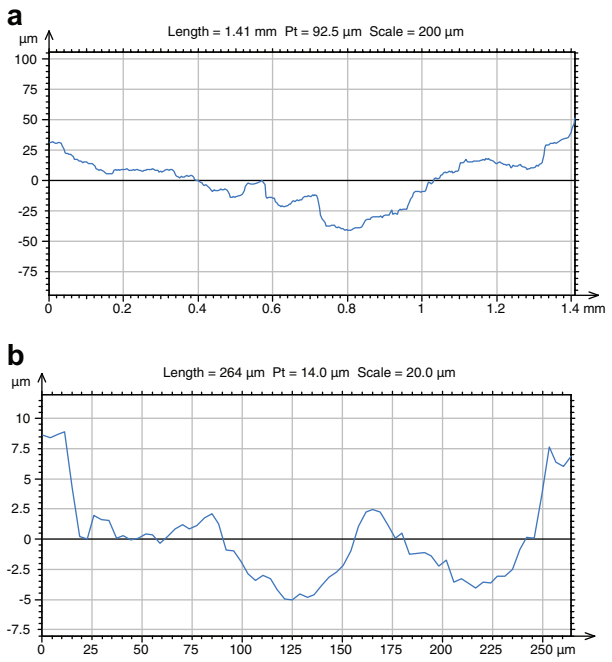

Fig 8. Example of self-similarity of roughness profile of worn metallic surface observed at different magnification. Profiles (**a**) and (**b**) present the same surface at different scale, AISI 1045, $P = 10$ N, $\delta^* = 150$ µm, $F = 15$ Hz, $N = 5{,}000$ cycles.

Conclusions

Dynamic evolution of surface roughness during friction and wear processes has been analyzed using first series of mirror polished Ti–6Al–4V samples and second series of samples with different initial roughness ($S_a = 0.282$–6.73 µm) prepared on Ti–6Al–4V and AISI 1045 samples.

Analysis of dynamic evolution of roughness during friction process shows that the degradation of material in abrasive wear process rapidly change the roughness in tribological contact. After an initial period of rapid degradation, condition of the interface will stabilize and roughness increase is much slower. However, analysis of initial roughness influence revealed that to certain extent a memory effect of interface exist and dynamic evolution of roughness will depend on initial condition and rheology of interface roughness evolution. Therefore, mechanical parts exposed to friction with poor initial finishing are susceptible to have much shorter lifetime than quality finished parts. This especially can concern the parts working under very severe contact conditions like rotor/blade contact, screws, clutch, etc.

Multiscale analysis shows that new surface created during abrasive wear process is rather uniform at different scales. That confirms that morphology created in wear process is composed from nano, micro, and macro scale roughness. Depending on specific application, initial surface morphology can be used to manage the friction and wear processes in more controllable way.

Nomenclature

F (Hz)	frequency of sinusoidal displacement
P (N)	normal load in contact
Q (N)	tangential load in contact
δ (µm)	relative displacement in contact
N	number of cycles in fretting test
S_q (µm)	root mean square height
S_{sk}	skewness
S_{ku}	kurtosis
S_p (µm)	maximum peak height
S_v (µm)	maximum pit height
S_z (µm)	maximum height
S_a (µm)	arithmetic mean height
S_{mc} (µm)	inverse areal material ratio
S_{xp} (µm)	extreme peak height
S_{pd} (1/mm^2)	density of peaks
S_{pc} (1/mm)	arithmetic mean peak curvature
S_{10z} (µm)	ten point height
S_{5p} (µm)	five point peak height
S_{5v} (µm)	five point pit height

Acknowledgement

K.J. Kubiak would like to thank all staff members of Laboratory TEMPO at the University of Valenciennes in France for inviting him to the laboratory, for financial support of this work and for very fruitful collaboration.

References

Bigerelle M, Mathia T, Bouvier S. 2012. The multi-scale roughness analyses and modeling of abrasion with the grit size effect on ground surfaces. Wear 286:124–135.

Bigerelle M, Van Gorp A, Gautier A, Revel P. 2007. Multiscale morphology of high-precision turning process surfaces. Proc Inst Mech Eng B J Eng Manuf 221:1485–1497.

Bouchbinder E, Procaccia I, Santucci S, Vanel L. 2006. Fracture surfaces as multiscaling graphs. Phys Rev Lett 96:055509.

Brown CA, Siegmann S. 2001. Fundamental scales of adhesion and area-scale fractal analysis. Int J Mach Tools Manuf 41:1927–1933.

Elliott D, Fisher J, Clark D. 1998. Effect of counterface surface roughness and its evolution on the wear and friction of PEEK and PEEK-bonded carbon fibre composites on stainless steel. Wear 217:288–296.

Fu YQ, Loh NL, Batchelor AW, et al. 1998. Improvement in fretting wear and fatigue resistance of Ti–6Al–4V by application of several surface treatments and coatings. Surf Coatings Technol 106:193–197.

Jerier JF, Molinari JF. 2012. Normal contact between rough surfaces by the Discrete Element Method. Tribol Int 47:1–8.

Kang MC, Kim JS, Kim KH. 2005. Fractal dimension analysis of machined surface depending on coated tool wear. Surf Coatings Technol 193:259–265.

Kasarekar AT, Sadeghi F, Tseregounis S. 2008. Fretting fatigue of rough surfaces. Wear 264:719–730.

Kubiak KJ, Liskiewicz TW, Mathia TG. 2011. Surface morphology in engineering applications: influence of roughness on sliding and wear in dry fretting. Tribol Int 44:1427–1432.

Kubiak K, Mathia T. 2009. Influence of roughness on contact interface in fretting under dry and boundary lubricated sliding regimes. Wear 267:315–321.

Kubiak K, Fouvry S, Marechal A. 2005. A practical methodology to select fretting palliatives: application to shot peening, hard chromium and WC-Co coatings. Wear 259:367–376.

Kubiak K, Fouvry S, Marechal A, Vernet J. 2006. Behaviour of shot peening combined with WC-Co HVOF coating under complex fretting wear and fretting fatigue loading conditions. Surf Coatings Technol 201:4323–4328.

Kubiak K, Mathia T, Fouvry S. 2010. Interface roughness effect on friction map under fretting contact conditions. Tribol Int 43:1500–1507.

Rapiejko C, Fouvry S, Grosgogeat B, Wendler B. 2009. A representative ex-situ fretting wear investigation of orthodontic arch-wire/bracket contacts. Wear 266:850–858.

Scott RS, Ungar PS, Bergstrom TS, et al. 2005. Dental microwear texture analysis within-species diet variability in fossil hominins. Nature 436:693–695.

Sokoloff JB. 2012. Surface roughness dry friction. Phys Rev E 85:027102.

Ungar PS, Brown CA, Bergstrom TS, Walker A. 2003. Quantification of dental microwear by tandem scanning confocal microscopy and scale-sensitive fractal analyses. Scanning 25:185–193.

Stahlmann J, Nicodemus ER, Sharma SC, Groche P. 2012. Surface roughness evolution in FEA simulations of bulk metal forming process. Wear 288:78–87.